

## NUMERICAL INVESTIGATION OF THE PARAMETRIC PENDULUM UNDER FILTERED RANDOM PHASE EXCITATION

Panagiotis Alevras<sup>1</sup>, Daniil Yurchenko<sup>1</sup>, and Arvid Naess<sup>2</sup>

<sup>1</sup>Department of Mechanical Engineering, Heriot-Watt University  
Edinburgh, EH14 4AS, UK  
e-mail: {pa132, d.yurchenko}@hw.ac.uk

<sup>2</sup> Department of Mathematical Sciences, NTNU  
Trondheim, NO 7491, Norway  
e-mail: arvidn@math.ntnu.no

**Keywords:** Narrow-band Parametric Excitation, Stochastic Modeling, Rotational Motion, Linear SDOF filter.

**Abstract.** *The parametrically excited pendulum is a highly nonlinear system which has been thoroughly studied regarding the response's stability and the fundamental types of motion that could be established. The rotating potential of a pendulum having its suspension point vertically excited was numerically identified and the appropriate excitation characteristics were presented. In this paper, the excitation is modeled using the random phase modulation and the rotational motion is sought. The resulting stochastic system is analyzed by using a numerical Path Integration (PI) method solving the Chapman-Kolmogorov equation to construct parameter space plots. The Probability Density Function (PDF) is computed and the rotational regions are identified as well as the effect of noise intensity onto them. Previous studies have shown that for small values of noise intensity the stochastic response resembles the deterministic one. However numerical simulations showed that with increasing noise intensity the regions of rotational motion become narrower. In order to improve the system's response a linear single-degree-of-freedom (SDOF) system is intercepted to filter the noisy excitation, forming a base excited SDOF system acting on the pendulum suspension point. The interaction between the moving pendulum mass and the SDOF filter is investigated with the goal being for the former to establish rotational motion.*

## 1 INTRODUCTION

Parametric excitation is a very well-known phenomenon that could be met in a variety of dynamical mechanical and electrical systems ([1, 2, 3]. These systems are often described as being internally excited since the excitation is inserted to the system through its parameters opposed to externally excited systems. In mechanical systems, such an excitation could be the result of changing stiffness, axial loading of a cantilever or vertical excitation of a pendulum's suspension point. In this paper, the parametric pendulum is considered. By applying Lagrange equations of the second kind in this case, the equation of motion would read:

$$ml^2\ddot{\theta} + \tilde{c}\dot{\theta} + mgl \sin \theta = ml\ddot{f}(t) \sin \theta \quad (1)$$

where  $\theta$  is the angle of inclination,  $\tilde{c}$  is the viscous damping coefficient,  $f(t)$  - excitation force,  $l$  - the length of the pendulum or the distance from the suspension point to the lumped mass  $m$ . If the excitation force is perfectly harmonic -  $f(t) = A \cos(\omega t)$  - then the previous equation may be rewritten:

$$\ddot{\theta} + c\dot{\theta} + \left[ \frac{g}{l} + \frac{A}{l}\omega^2 \cos(\omega t) \right] \sin \theta = 0 \quad (2)$$

The fraction  $g/l$  is usually notated as  $\Omega^2$ , with  $\Omega$  being the natural frequency of the linearized system. When it comes to linearizing equation (2) by considering a small angles approximation -  $\sin \theta \approx \theta$  - the damped widely known Mathieu equation is derived:

$$\ddot{\theta} + c\dot{\theta} + \left[ \Omega^2 + \frac{A}{l}\omega^2 \cos(\omega t) \right] \theta = 0 \quad (3)$$

Applying the Floquet theory [2], the above equation (3) can be proved to have both bounded and unbounded solutions. Returning to the actual pendulum equation (2) a much colorful response exists. Asymptotically stable, periodic oscillatory, rotational and even chaotic motion can be observed. Numerous studies [4, 5, 6, 7, 8] were devoted to determining the stability-instability boundaries by different methods such as Lyapunov exponents, perturbation analysis, bifurcation analysis and other. Introducing non-dimensionalization of the time domain,  $\tau = \Omega t$ , transforms the studied equation (2):

$$\begin{aligned} \theta'' + \gamma\theta' + [1 + \lambda \cos(\nu\tau)] \sin \theta &= 0, \\ \tau = \Omega t, \quad \Omega^2 = \frac{g}{l}, \quad \nu = \frac{\omega}{\Omega}, \quad \lambda = \frac{A}{l}\nu^2 = \frac{A\omega^2}{g} \end{aligned} \quad (4)$$

where the prime denotes differentiation with respect to  $\tau$  and  $\gamma$  is the scaled damping coefficient.

In [8], approximate analytical solutions were derived for equation (4) and the boundaries of the stability region were approximated. The resonance zones, with the first resonance region at a frequency ratio  $\nu = \omega/\Omega = 2$  being the most important, introduce period doubling bifurcations which result in generation of period-two oscillations. Increasing the amplitude of the excitation makes rotations of period-one and period-two achievable as well as introducing the system into a region of chaos. In [9] and [10] parameter space plots were constructed classifying the response according to not only the stability but the type of the response as well.

In this paper, the scope is concentrated on identifying the rotational regions only. Such an interest is motivated by a recently proposed concept [9, 11] for a Wave Energy Converter that would utilize the wave bobbing motion to provide the vertical excitation to the discussed parametric pendulum. The rotational response is much more preferable for generating electricity from oscillatory or chaotic motion because of the higher energy levels of the motion and the

reliability of the device respectively. Thus, the basic tool here is parameter space plots characterizing the amount of rotations experienced by the pendulum. Up to this point, the dynamical systems considered are deterministic since the excitation  $f(t)$  was considered purely periodic. However, this is reductive of the real-world environment, since ocean waves are not purely periodic and should be rather modeled as a narrow-band stochastic process. Throughout this paper, random phase modulation is incorporated into the parametric excitation, as proposed by Wedig [12], describing the real-world phenomena in a more realistic way. So, instead of the purely sinusoidal function, the previous randomness provides the excitation as:

$$f(t) = A \cos q, \quad \dot{q} = \omega + \tilde{\sigma} \zeta(t) \quad (5)$$

where  $\zeta(t)$  is a Gaussian White Noise of  $D = \tilde{\sigma}^2$  intensity for which:

$$E[\zeta(t)] = 0, \quad E[\zeta(t)\zeta(t + \rho)] = D\delta(\rho) \quad (6)$$

This formulation leads to the following system:

$$\begin{aligned} \theta'' + \gamma\theta' + (1 + \lambda \cos q) \sin \theta &= 0 \\ q' &= \nu + \sigma \zeta(\tau) \end{aligned} \quad (7)$$

Equation (7) is strongly nonlinear, for which an analytical approach would be much more difficult to be applied even for the deterministic system. Thus, a numerical approach is adopted dealing with the discrete dynamical system:

$$\begin{aligned} x_1 &= x'_1 + x'_2 \Delta\tau \\ x_2 &= x'_2 - \gamma x'_2 \Delta\tau - [1 + \lambda \sin x'_3] \sin x'_1 \Delta\tau \\ x_3 &= x'_3 + \nu \Delta\tau + \sigma \Delta W(\tau) \end{aligned} \quad (8)$$

where  $x_1$  represents the angle,  $x_2$  the angular velocity,  $x_3$  the excitation phase,  $\sigma = \tilde{\sigma}/\Omega$ ,  $\Delta\tau$  the scaled discretization time step, the prime stands for the previous time step and  $\Delta W(\tau) = W(\tau) - W(\tau - \Delta\tau)$  is a standard Wiener process. Note that formally, the Wiener process is not differentiable. However, it has been observed in particle physics and the Brownian motion of particles that the following approximation is rather representative,  $\zeta(t)\Delta t = \Delta W(t)$ . In the discretized equation (8) a simple Euler-Maruyama scheme has been applied. In order to increase the accuracy of the solution a 4<sup>th</sup> order Runge-Kutta-Maruyama scheme is adopted which utilizes the widely known Runge-Kutta techniques instead of the Euler one.

A widely used technique for analyzing equations (8) is the Monte-Carlo (MC) simulations. These include sampling of the stochastic response process and statistical exploitation of the results. These methods require a random number generator and usually a number of realizations is performed. The nowadays high computing capabilities make such techniques rather quick. However, due to their sampling nature they are always reductive. In this paper, a numerical Path Integration (PI) method [13] is implemented based on invoking the total probability law:

$$p(\mathbf{x}, t) = \int_{-\infty}^{\infty} \int_{-\infty}^{\infty} \int_{-\pi}^{\pi} p(\mathbf{x}, t | \mathbf{x}', t') p(\mathbf{x}', t') d\mathbf{x}'. \quad (9)$$

where  $\mathbf{x}$  is the variables vector,  $p(\mathbf{x}, t)$  is the joint probability density function (PDF) at time  $t$  and  $p(\mathbf{x}, t | \mathbf{x}', t')$  is the transitional probability density function (TPD). The method applies

an iterative approach by moving an initial PDF forward in time up until the point where the stationary solution is obtained. The TPD function in the case of equation (8) takes the following form:

$$p(\mathbf{x}, t|\mathbf{x}', t') = \delta(x_1 - x'_1 - r_1(\mathbf{x}', \Delta t))\delta(x_2 - x'_2 - r_2(\mathbf{x}', \Delta t))\tilde{p}(x_3, t|x'_3, t') \quad (10)$$

where  $\delta$  denotes the Dirac function and  $r_i$  stands for the Runge-Kutta evolution of the  $i^{th}$  variable. Since the stochastic excitation is of Gaussian nature and is inserted to the system only by the last equation, the former equation includes:

$$\tilde{p}(x_3, t|x'_3, t') = \frac{1}{\sqrt{2\pi D\Delta t}} \exp\left(-\frac{(x_3 - x'_3 - r_3(\mathbf{x}', \Delta t))^2}{2D\Delta t}\right) \quad (11)$$

The PI method has been used and proved very efficient for constructing the PDFs of different, even strongly nonlinear, systems [14, 15] as well as some reliability problems [16, 17]. In [18], both MC methods and the PI method were used to analyze equation (8). The effect of increasing noise onto the rotational response of the parametric pendulum was investigated. Parameter space plots, figure 1, were constructed characterizing the amount of rotational motion. Particularly, red stands for  $> 90\%$  and blue for  $< 10\%$ , counting different types and directions of rotations as one [18].

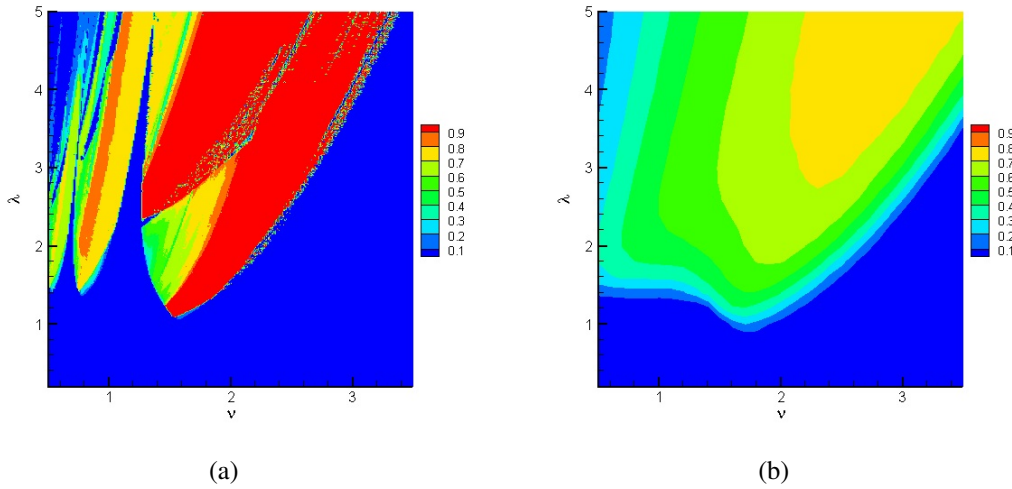


Figure 1: Parameter space plot with ratio of rotational motion for  $\gamma = 0.3$  and  $y(0) = 0$ . (a)  $D = 0.0$ ; (b)  $D = 0.3$ ;

As it can be seen from figures 1(a) and 1(b) increasing the noise intensity causes the rotational motion to drop from purely rotational response to around 75%. Even though such an amount cannot be considered as negligible, different ways to enhance the rotational motion in a random environment are sought. In the following, a linear single-degree-of-freedom spring-mass-damper system is intercepted between the excitation and the pendulum, acting as a noise filter and their coupled dynamics are investigated.

## 2 LINEAR SDOF FILTER

A linear SDOF system is proposed to filter the vertical stochastic excitation acting on the pendulum's suspension point as depicted in figure 2. The system constitutes of a base-excited

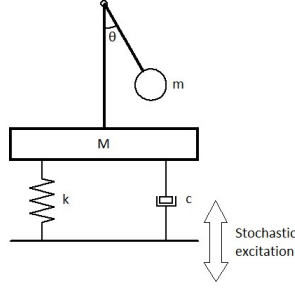


Figure 2: Sketch of the parametrically excited pendulum of mass  $m$  through a base-excited linear SDOF system of mass  $M$ .

linear SDOF system and the parametrically excited pendulum. The following system of differential equations describe the coupled dynamics:

$$\begin{aligned} \ddot{\theta} + c\dot{\theta} + (\Omega^2 - \ddot{x}/l) \sin \theta &= 0 \\ \ddot{x} + 2\alpha\dot{x} + \eta^2 x &= \eta^2 A \cos q(t) - 2\alpha\omega A \sin q(t) + g + \frac{m}{M+m} l \ddot{\theta} \sin \theta + \frac{m}{M+m} l \dot{\theta}^2 \cos \theta \quad (12) \\ \dot{q}(t) &= \omega + \tilde{\sigma}\zeta(t) \end{aligned}$$

where  $\omega$  - the mean excitation frequency,  $A$  - the excitation amplitude,  $\alpha$  - the linear system's damping coefficient,  $\eta$  - its natural frequency and  $M$  - the total mass of the secondary SDOF system. Applying the same time non-dimensionalization as before,  $\tau = \Omega t$ , as well as setting  $y = x/l$ ,  $m_r = m/(M + m)$  and using the definitions  $\nu = \omega/\Omega$ ,  $\lambda = A\nu^2/l$ , the filter's scaled natural frequency  $e = \eta/\Omega$  and the scaled damping coefficient  $\beta = \alpha/\Omega$ , equations (12) become:

$$\begin{aligned} \theta'' + \gamma\theta' + (1 - y'') \sin \theta &= 0 \\ y'' + 2\beta y' + e^2 y &= \frac{e^2 \lambda}{\nu^2} \cos q - \frac{2\beta \lambda}{\nu} \sin q + 1 + m_r \theta'' \sin \theta + m_r \theta'^2 \cos \theta \quad (13) \\ q' &= \nu + \sigma\zeta(\tau) \end{aligned}$$

In the case of  $m \ll M$  then  $m_r \approx 0$  and thus the two last terms in the RHS of the system's (12) second equation might be omitted. Then the linear system is a typical base-excited SDOF system having random exciting phase. Furthermore, from basic trigonometry, the remaining sinusoidal terms in the RHS of the same equation could as well be represented by an imperfect harmonic function, say  $g(\tau) = A^* \sin(q + \phi)$ . Among other, the PI method has also been used to analyze this system, calculating the joint PDF of the response and its derivative.

Moreover, in [19], the coupled system described as in equation (13) has been studied with regard to the rotational motion of the pendulum when the random excitation is filtered, assuming that the mass ratio is negligible. That is, no influence of the pendulum onto the linear SDOF system was taken into account. Figure 3 compares the rotation-wise response of the pendulum alone with the one of the coupled system's. In both figures 3(a) and 3(b), the provided vertical excitation is the same meaning that the parameter pair  $(\nu, \lambda)$  describes the characteristics of the random phase excitation. In that way, the addition of the linear SDOF system was able to be evaluated. Comparing the level of rotational motion in these two figures, it is obvious that the addition of linear SDOF system is extremely beneficiary for establishing and maintaining the rotational response. In figure 3(a) the corresponding value is only 75% while in figure 3(b) the same value is  $> 90\%$  with the shape and position of the maximal rotational region having been changed and brought at a lower amplitude level. Of course, changing the natural

frequency of the linear SDOF filter or the value of its damping coefficient will change the response significantly providing another option for controlling the system as well, but such a discussion exceeds the scope of this paper.

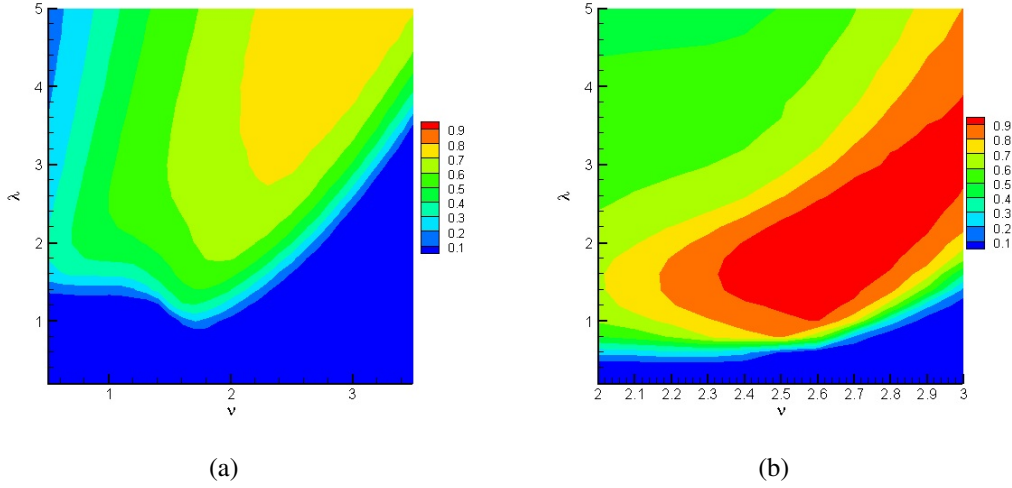


Figure 3: Parameter space plot with ratio of rotational motion for  $D = 0.3$ ,  $\gamma = 0.3$ . (a) without filter; (b) with filter and  $e = 2.5$ ,  $\beta = 0.3$ ,  $m_r = 0$ ;

Also, one could notice that the parameter space plot in figure 3(b) is extended to a shorter range at the  $\nu$  axis. This is because the response of the linear filter will retain the narrow-band property of the excitation only under certain conditions, one of which is low detuning value between the excitation frequency  $\omega$  and the system's natural one  $\eta$ .

### 3 INFLUENCE OF PENDULUM'S MASS

In this section, the rotational motion of the pendulum is investigated when the influence of its mass  $m$  onto the response of the linear SDOF filter cannot be neglected. The problem now is formulated by the full equations (13) and the parameter  $m_r$  becomes a subject of study. Figure 4 shows parameter space plots characterizing the amount of rotational motion in the same way as in figure 3(b). The left column of the plots depicts the numerical results for the value of damping coefficient,  $\beta = 0.1$ , while the right column for  $\beta = 0.5$ . A first observation can be made with regard to the influence of the damping coefficient,  $\beta$ . Considering that the natural frequency of the linear SDOF filter is  $e = 2$ , the filter is a system at or around its resonance. When the  $\beta$  value is small, the amplification of the response leads it to very high amplitude values forcing the pendulum to move closer to the region above the rotational one, thus reducing the rotational amount in comparison with the higher  $\beta$  values. The latter values drive the pendulum inside the rotational parameter region providing a better response for the pendulum to rotate. Obviously, there is a critical damping value, larger ones than which get the filter's response smaller in amplitude up until the point it dies out.

Furthermore, the plots in the same line present results for the same mass ratio,  $m_r$ . Figures 4(a) and 4(b) correspond to cases with  $m_r = 0$  and have been added for comparison purposes. When the mass ratio gets slightly bigger, and particularly equal to  $m_r = 0.1$  shown in figures 4(c) and 4(d), the whole plots resemble the ones without the pendulum's influence (figures 4(a) and 4(b)), with the only difference being a slight increase in the experienced rotational motion.

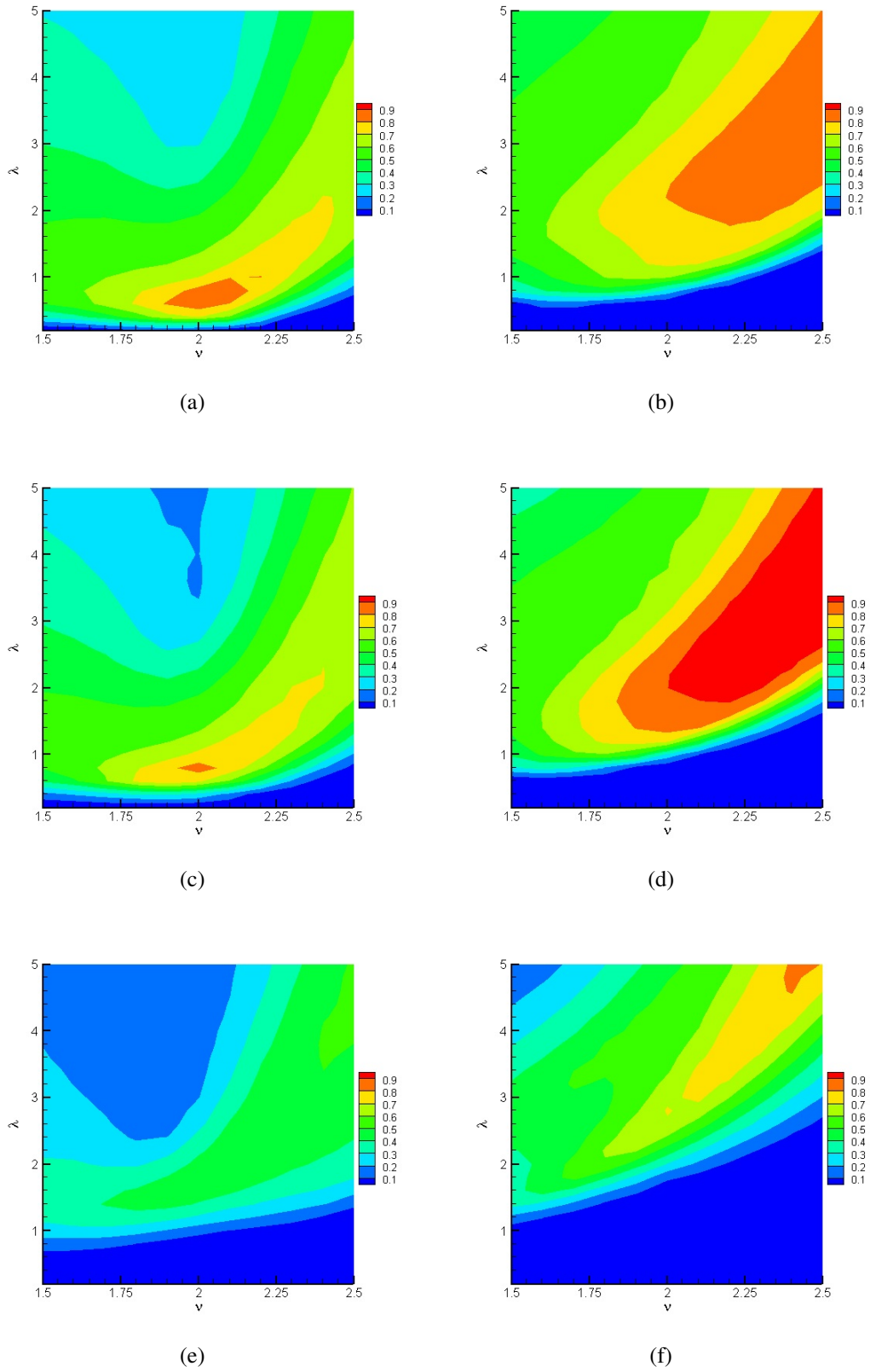


Figure 4: Parameter space plot with ratio of rotational motion for  $D = 0.3, \gamma = 0.3, e = 2$ . (a)  $m_r = 0.0, \beta = 0.1$ ; (b)  $m_r = 0.0, \beta = 0.5$ ; (c)  $m_r = 0.1, \beta = 0.1$ ; (d)  $m_r = 0.1, \beta = 0.5$ ; (e)  $m_r = 0.5, \beta = 0.1$ ; (f)  $m_r = 0.5, \beta = 0.5$ ;

However, when the value of the mass ratio gets even higher, as in figures 4(e) and 4(f) for which the pendulum mass equals the filter's, the response of the pendulum contains less rotations than before, keeping nevertheless at the appropriate damping conditions a respectable amount of around 75% in place. Also, it is observed that some lower amplitudes points of the plot get stabilized, turning into blue asymptotically or marginally stable points.

#### 4 CONCLUSIONS

The coupled dynamics of a parametric pendulum vertically excited by a random phase imperfect harmonic function were in question. The characteristics of the excitation were improved by filtering it through a linear SDOF system acting at small detuning values. The effect of the filter on the pendulum's rotational motion has proven beneficiary when the pendulum's mass is very much smaller than the filter's. In this paper, the latter assumption is removed and the influence of the pendulum's mass onto the response of the linear SDOF filter is investigated. As it was seen through the numerical construction of parameter space plots, small values of the ratio of the pendulum's mass over the filter's slightly enhance the rotational motion, while when these masses are equal the desired response decreases. However, the rotational motion is still maintained even at a lower level, around 75%, when the damping coefficient is chosen properly. The latter also gives rise to the option of using the filter for controlling purposes as well.

#### REFERENCES

- [1] Y.K. Lin, G.Q. Cai, *Probabilistic Structural Dynamics*, McGraw-Hill, New York, 1995.
- [2] A.H. Nayfeh, D.T. Mook, *Nonlinear Oscillations*, Wiley, New York, 1979.
- [3] K.L. Turner, S.A. Miller, P.G. Hartwell, N.C. MacDonald, S.H. Strogatz, S.G. Adams, Five parametric resonance in a MEMs, *Nature*, **396**, 149-152, 1998.
- [4] M.J. Clifford, S.R. Bishop, Rotating periodic orbits of the parametrically excited pendulum, *Physics Letters A*, **201**, 191-196, 1995.
- [5] R.W. Leven, B.P. Koch, Chaotic behavior of a parametrically excited damped pendulum, *Physics Letters A*, **86**, 71-74, 1981.
- [6] R.W. Leven, B. Pompe, C. Wilke, B.P. Koch, Experiments on periodic and chaotic motions of a parametrically forced pendulum, *Physica D*, **16**, 371-384, 1985.
- [7] W. Szemplinska-Stupnicka, E. Tyrkiel, The Oscillation-rotation attractors in the Forced Pendulum and their Peculiar Properties, *International Journal of Bifurcation and Chaos*, **12**(1), 159-168, 2002.
- [8] X. Xu, M. Wiercigroch, Approximate analytical solutions for oscillatory and rotational motion of a parametric pendulum, *Nonlinear Dynamics*, **47**, 311-320, 2007.
- [9] X. Xu, M. Wiercigroch, M.P. Cartmell, Rotating orbits of a parametrically-excited pendulum, *Chaos, Solitons & Fractals*, **23**, 1537-1548, 2005.
- [10] B.W. Horton, J. Sieber, J.M.T. Thomson and M. Wiercigroch, Dynamics of the nearly parametric pendulum. *International Journal of Non-Linear Mechanics*, **46**(2), 436-442, 2011.



- [11] S. Lenci, M. Brocchini, C. Lorenzoni, Experimental rotations of a pendulum on water waves, *Journal of Computational and Nonlinear Dynamics*, **7**, 011007 (9 pages), 2012.
- [12] W.V. Wedig, Invariant measures and Lyapunov exponents for generalized parameter fluctuations, *Structural Safety*, **8**, 13-25, 1990.
- [13] A. Naess, V. Moe, Efficient path integration methods for nonlinear dynamic systems, *Probabilistic Engineering Mechanics*, **15**, 221-231, 2000.
- [14] D.V. Iourtchenko, A. Naess, E. Mo, Response probability density functions of strongly nonlinear systems by the path integration method, *International Journal of Non-linear Mechanics*, **41**, 693-705, 2006.
- [15] A. Naess, F.E. Kolnes, E. Mo, Stochastic spur gear dynamics by numerical path integration, *Journal of Sound and Vibrations*, **302**, 936-950, 2007.
- [16] D.V. Iourtchenko, E. Mo, A. Naess, Reliability of strongly nonlinear SDOF dynamic systems by the path integration method, *Journal of Applied Mechanics*, **75**, 2008.
- [17] A. Naess, D.V. Iourtchenko, O. Batsevych, Reliability of systems with randomly varying parameters by the path integration method, *Probabilistic Engineering Mechanics*, **26**, 5-9, 2011.
- [18] D. Yurchenko, A. Naess, P. Alevras, Pendulum's rotational motion governed by a stochastic Mathieu equation, *Probabilistic Engineering Mechanics*, **31**, 12-18, 2013.
- [19] D. Yurchenko, P. Alevras, Stochastic Dynamics of a parametrically base excited rotating pendulum, *Procedia IUTAM* (2012), to be published.